ISSN 2616-5880 Vol. 5, Issue 2: 37-45, DOI: 10.25236/AJMC.2024.050207

Preparation of Activated Carbon Materials from Coal Gasification Ash and Removal of Complexed Copper

Miao Jiahui

School of Environmental Science and Engineering, Nanjing University of Information Science & Technology (NUIST), Nanjing, Jiangsu, China
2321178012@qq.com

Abstract: *The wastewater containing complexed copper produced by chemical copper plating has always been a challenge in industrial wastewater treatment. Activated carbon, with its high strength, developed porosity, and large specific surface area, is widely used in the field of electroplating wastewater treatment. This study uses solid waste gasification ash as raw material and prepares activated carbon, investigating its adsorption performance and influencing factors on copper ions and complexed copper ions. The results show that the activated carbon from coal gasification ash (AC) has different adsorption effects on Cu^{2+}, copper-ammonia complex (Cu-NH_3), copper-citrate complex (Cu-Cit), and copper-EDTA complex (Cu-EDTA), with the adsorption capacity being in the order of Cu^{2+} > Cu-EDTA > Cu-NH_3 > Cu-Cit, and their respective adsorption capacities are 40.94, 33.98, 28.87, and 23.70 mg/g. The adsorption process of AC on Cu^{2+}, Cu-NH_3, Cu-Cit, and Cu-EDTA is more consistent with the second-order kinetic model, and the adsorption isotherm is more in line with the Langmuir model. Characterization methods such as Scanning Electron Microscopy (SEM), Specific Surface Area measurement (BET), X-Ray Diffraction (XRD), Energy Dispersive X-ray Spectroscopy (EDX), and Fourier Transform Infrared Spectroscopy (FTIR) indicate that AC mainly presents an irregular shape, with a certain amount of porosity on the surface; it has a large specific surface area and contains a large number of functional groups such as hydroxyl groups on the surface.*

Keywords: *Adsorption; Activated carbon from coal gasification ash; complexed copper*

1. Introduction

In industrial production, industries such as electroplating and printed circuit board manufacturing are the main sources of wastewater containing copper[1]. In these industries, copper in the wastewater primarily exists in a complexed form[2], which is more difficult to treat than ionic copper. Coal gasification ash is a solid residue formed during the incomplete combustion of coal with oxygen or oxygen-enriched air to produce CO and H_2[3], where the inorganic minerals in coal undergo various physicochemical transformations along with residual carbon particles in the coal. China is a country with an energy structure dominated by coal[4]. In 2018, China's raw coal output was 3.68 billion tons, and consumption was 3.9 billion tons, accounting for 69.6 % and 59 % of the primary energy production and consumption, respectively, thus generating a large amount of coal gasification ash annually. Currently, the main disposal methods for coal gasification ash in China are landfilling and storage[5], which may cause serious environmental pollution, and landfilling and storage also lead to a significant waste of land resources, necessitating a more reasonable method to dispose of coal gasification ash[6].

Adsorption is an efficient method for the removal of heavy metals utilizing the unique porous structure of adsorbents. Adsorbents used in the treatment of electroplating heavy metal wastewater by adsorption include polysaccharide resins, banana peels, etc. Xu et al. prepared a type of amino-modified attapulgite that can be used to adsorb Cu^{2+} in the liquid phase[7]. Activated carbon is simple to prepare and is widely used in the treatment of wastewater containing heavy metals, but its regeneration efficiency is low, and it is difficult to meet the requirements for reuse after treatment. Currently, the high cost of adsorbents commonly used in the industrial field limits the widespread application of adsorption. Therefore, developing efficient and inexpensive water treatment adsorbents is an important direction in adsorption research[8].

This study uses gasification ash as the experimental material to prepare activated carbon adsorbents, providing a theoretical basis for the preparation of cost-effective adsorbents and the resource utilization

ISSN 2616-5880 Vol. 5, Issue 2: 37-45, DOI: 10.25236/AJMC.2024.050207

of coal gasification ash. With Cu in wastewater as the target for removal, the study investigates the adsorption performance of activated carbon from coal gasification ash on wastewater containing copper, thereby providing theoretical support for the removal of heavy metals from wastewater using coal gasification ash and enabling its wide application.

2. Materials and methods

2.1 Materials and chemicals

Copper sulfate ($CuSO_4 \cdot 5H_2O$, ≥99.8 %), Ammonia (NH_3, ≥99.9 %), Trisodium citrate ($C_6H_5Na_3O_7$, ≥99.9 %), Disodium ethylenediaminetetraacetic acid ($C_{10}H_{14}N_2Na_2O_8$, ≥99.9 %), Nitric acid (HNO_3, 68.0 %), Perchloric acid ($HClO_4$, 72 %), Provided by Shanghai Macklin Biochemical Technology Co., Ltd., all reagents are of analytical grade (AR).

2.2 Experimental methods

2.2.1 Preparation of activated carbon from coal gasification ash

The collected coal gasification ash consists of slag particles with diameters ranging from 0.5 to 5.0 millimeters, and its main components are as shown in Table 1.

Table 1: Main components of activated carbon from coal gasification ash.

Ingredient	SiO_2	Al_2O_3	Fe_2O_3	CaO	MgO	Other
Content(%)	39.67	26.77	12.80	9.96	2.43	8.37

AC is produced by air-drying, pulverizing, pyrolyzing, and sieving the gasification slag. It appears as a fine, uniform black powder. The collected gasification slag is ground with a mortar and passed through a 100-mesh sieve, then packed into a self-sealing bag, labeled, and placed in a desiccator for later use.

2.2.2 Experimental method for activated carbon from coal gasification slag

(1) Adsorption isotherm experiment

Prepare 50 mL of four stock solutions with concentrations of 5, 10, 20, 30, 60, and 80 mg/L of Cu^{2+}, Cu-NH_3, Cu-Cit, and Cu-EDTA, respectively. Add 20 mg of activated carbon from coal gasification slag to each, and shake for 24 hours. After settling to equilibrium, take the supernatant, acidify with 2 mL of nitric acid, filter through a 0.45 μm filter membrane, and determine the concentration of copper ions in the filtrate using an atomic absorption spectrophotometer.

(2) Adsorption kinetics experiment

Prepare 50 mL of 10 mg/L solutions of Cu^{2+}, Cu-NH_3, Cu-Cit, and Cu-EDTA, respectively. Add 20 mg of activated carbon from coal gasification slag to each, and set adsorption times for 60, 120, 240, 480, 720, and 1440 minutes. After each time interval, take the supernatant after settling to equilibrium. After that, the experimental steps are the same as above.

(3) Effect of pH on adsorption experiment

Prepare six sets of 50 mL of 10 mg/L Cu^{2+} solution, add 20 mg of activated carbon from coal gasification slag to each, and adjust the pH to 2.0, 3.0, 4.0, 5.0, 6.0, 7.0, and 8.0, respectively. After shaking for 24 hours, remove and allow to settle to equilibrium, then take the supernatant. After that, the experimental steps are the same as above.

(4) Effect of Dosage on adsorption experiment

Prepare six sets of 50 mL of 10 mg/L Cu^{2+} solution, and add varying amounts of activated carbon from coal gasification slag: 20, 40, 60, 80, and 100 mg, respectively. After shaking for 24 hours, remove and allow to settle to equilibrium, then take the supernatant. After that, the experimental steps are the same as above.

2.3 Data analysis

Origin7.5 software is used for fitting and analyzing the experimental data. All experimental

ISSN 2616-5880 Vol. 5, Issue 2: 37-45, DOI: 10.25236/AJMC.2024.050207

processes are conducted with three parallel samples, and their average values are taken as the final results. The adsorption data analysis models and parameters are shown in Table 2.

Table 2: Adsorption data analysis models and parameters.

Type of calculation	Mathematical expression	Meaning of parameters
Calculation of adsorption quantity	$q_e = \frac{(C_0 - C_e)V}{W}$ $q_t = \frac{(C_0 - C_t)V}{W}$	q_e is equilibrium adsorption capacity (mg· g^{-1}); q_t is adsorption capacity at time t (mg· g^{-1}); V is volume of the Cu^{2+} solution (mL); W is dosage of the adsorbent (mg).
Pseudo-first-order adsorption kinetics[9]	$\ln(q_e - q_t) = \ln q_e - k_1 t$	k_1 is adsorption rate constant (min^{-1}).
Pseudo-second-order adsorption kinetics[9]	$\frac{t}{q_t} = \frac{1}{k_2 q_e^2} + \frac{t}{q_e}$ $h_0 = k_2 q_e^2$	k_2 is adsorption rate constant (g·mg^{-1}· min^{-1}); h_0 is initial adsorption rate (mg·g^{-1}· min^{-1}); q_m is maximum adsorption capacity for monolayer coverage (mg· mg^{-1}); C_e is concentration of the adsorbate in the liquid phase at equilibrium (mg·L^{-1}).
Langmuir model[10]	$\frac{C_e}{q_e} = \frac{1}{bq_m} + \frac{C_e}{q_m}$	b is adsorption equilibrium constant related to adsorption heat (L·mg^{-1}); K_F is Freundlich constant related to adsorption capacity [(mg/g)(L/mg)^n].
Freundlich model[10]	$q_e = K_F C_e^{1/n}$	n is constant related to the intensity of adsorption.

3. Results and discussion

3.1 Scanning electron microscope analysis

Using the Shimadzu SSX550 scanning electron microscope to analyze the activated carbon from coal gasification slag allows for a clear and direct observation of the sample's microporous structure, as shown in Figure 1.

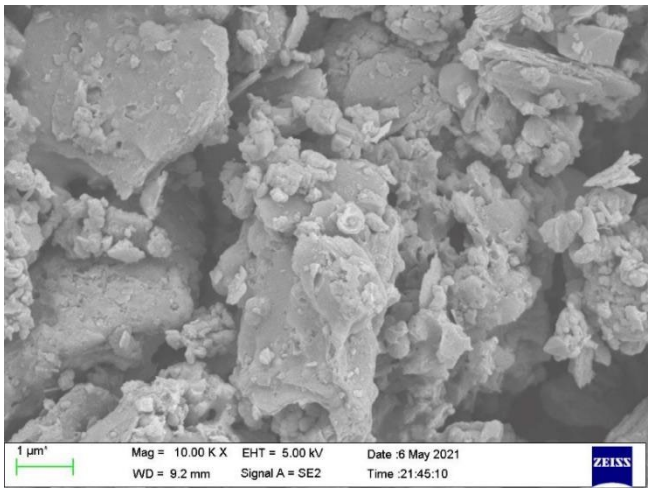

Figure 1: SEM image of AC.

The electron microscope image of the coal gasification slag reveals that the activated carbon primarily exhibits an irregular glassy phase. The surface of the irregular structure is relatively rough and contains a certain amount of porosity; it also includes a mixture of some spherical particles. The surface of the spherical particles is relatively smooth[11], mainly because they are formed under high-temperature melting conditions.

ISSN 2616-5880 Vol. 5, Issue 2: 37-45, DOI: 10.25236/AJMC.2024.050207

3.2 Specific surface area analysis

At -196 ºC, the specific surface characteristics of the sample are determined using an analyzer. The sample is first pretreated at 200 ºC, and the measurement type is total pore measurement, followed by calculation. The table 3 below shows the specific surface area of AC.

Table 3: Specific surface area of AC.

Sample	BET (m^2/g)	PV (cm^3/g)	PS (Å)
AC	147.915	0.098	27.052

From this table, it is known that the specific surface area of AC is 147.915 m²/g, the pore volume is 0.098 cm³/g, and the PS is 27.052. This indicates that AC contains a relatively rich pore structure. According to the research by Liu[12], after the carbon in AC is removed, the pore structure also largely disappears, leading to the conclusion that the porous structure of AC is primarily provided by the incompletely combusted carbon within it.

3.3 EDX energy spectrum analysis

An EDX energy spectrum analysis is performed on the framed area in the SEM image shown in Figure 2, resulting in the energy spectrum and main element ratios of the activated carbon from coal gasification slag and modified coal gasification slag as shown in Table 4.

The EDX energy spectrum and elemental content analysis table reveal that the main element in AC is carbon, with a percentage content of 84.17%. This indicates that carbon plays a dominant role in the adsorption process, leading to a significant adsorption effect. Additionally, the amount of oxygen contained in AC is relatively high. The likely reason is that during the high-temperature pyrolysis process of AC, there was no nitrogen protection, allowing a small amount of air to enter and participate in the high-temperature pyrolysis process[13].

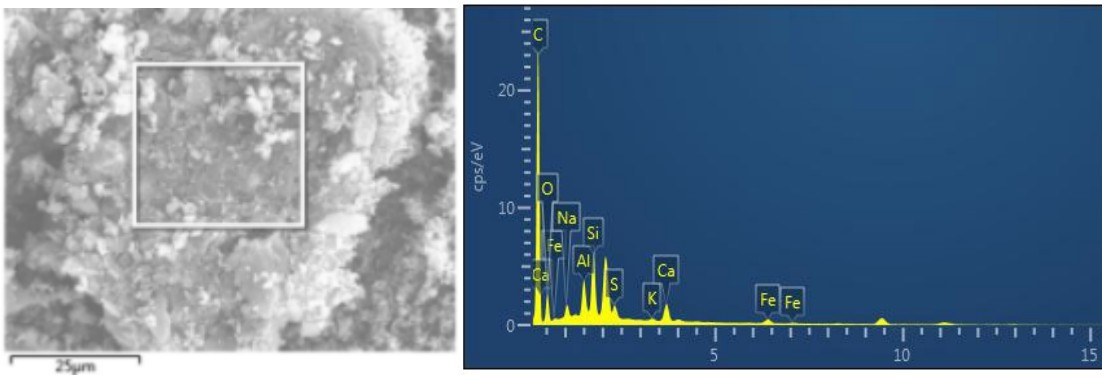

Figure 2: Energy spectrum image of AC.

Table 4: Main element ratios of AC.

Elements	Wt %	Atomic percentage %
C	75.44	84.17
O	12.91	10.81
Na	1.17	0.68
Al	2.06	1.02
Si	3.74	1.78
S	1.09	0.45
K	0.25	0.08
Ca	1.94	0.65
Fe	1.40	0.34
Total	100.00	100.00

ISSN 2616-5880 Vol. 5, Issue 2: 37-45, DOI: 10.25236/AJMC.2024.050207

3.4 Adsorption isotherms

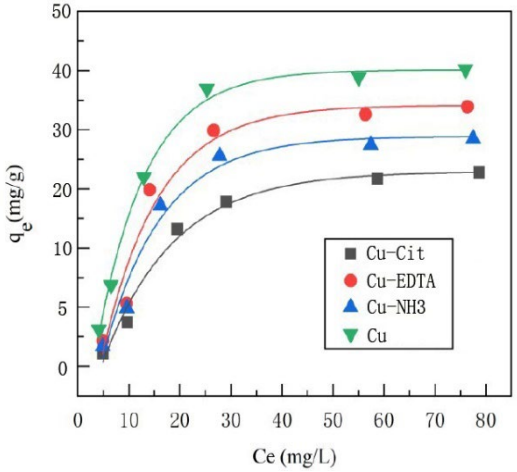

Figure 3: Adsorption isotherms of AC for Cu^{2+}, Cu-NH_3, Cu-Cit, and Cu-EDTA.

Figure 3 shows the adsorption isotherms of activated carbon from coal gasification slag for Cu^{2+}, Cu-NH_3, Cu-Cit, and Cu-EDTA. As the initial concentration increases, the adsorption rate of the activated carbon for Cu^{2+}, Cu-NH_3, Cu-Cit, and Cu-EDTA increases rapidly, followed by a slow rise. This is because the number of adsorbent sites is limited. At the initial concentration, the adsorbent sites are filled. As the concentration gradually increases, the sites are more fully utilized until no further filling is possible, thus reaching equilibrium.

Figures 4 (a) and (b) represent the Langmuir and Freundlich adsorption isotherm graphs for the adsorption of Cu^{2+}, Cu-NH_3, Cu-Cit, and Cu-EDTA by activated carbon from coal gasification slag, respectively. According to Table 5, the adsorption of Cu^{2+}, Cu-NH_3, Cu-Cit, and Cu-EDTA by activated carbon from coal gasification slag fits better with the Langmuir adsorption isotherm, with corresponding R^2 values of 0.986, 0.997, 0.993, and 0.995, respectively.

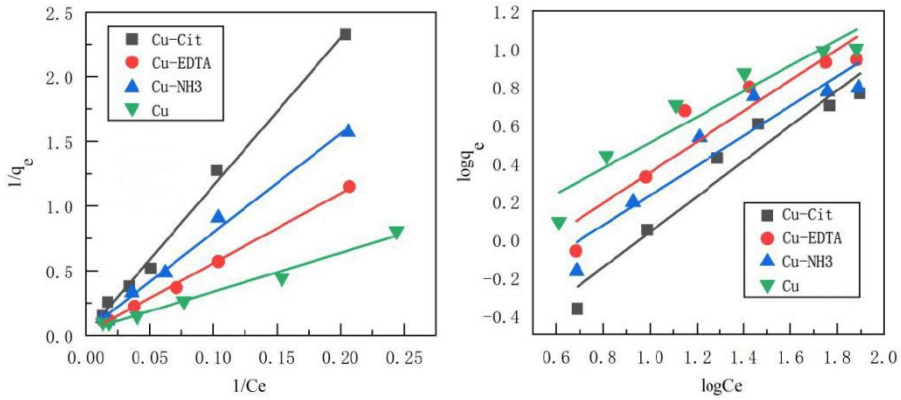

Figure 4: Langmuir and Freundlich isotherms for the adsorption of Cu^{2+}, Cu-NH_3, Cu-Cit, and Cu-EDTA.

Table 5: Isotherm parameters for the adsorption of Cu^{2+}, Cu-NH_3, Cu-Cit, and Cu-EDTA by AC.

Adsorbent	Langmuir Isotherm Parameters			Freundlich Isotherm Parameters		
	Q^0/mg·g^{-1}	b/L·mg^{-1}	R^2	K_F	n	R^2
AC	40.94	0.0123	0.9860	0.6789	1.4880	0.9047
AC-EDTA	33.98	0.0034	0.9970	0.3545	1.2407	0.8808
AC-NH_3	28.87	0.0041	0.9930	0.2867	1.2804	0.8778
AC-Cit	23.70	0.0011	0.9950	0.1302	1.0788	0.9376

ISSN 2616-5880 Vol. 5, Issue 2: 37-45, DOI: 10.25236/AJMC.2024.050207

3.5 Adsorption kinetics

To study the adsorption process of the adsorbent material for Cu2+, Cu-NH3, Cu-Cit, and Cu-EDTA, the Lagergren first-order reaction kinetics model and the second-order reaction kinetics model are used to fit the experimental data of the adsorbent material for Cu2+, Cu-NH3, Cu-Cit, and Cu-EDTA. The Lagergren first-order reaction rate equation is:

$$\log(q_e - q_t) = \log q_e - \frac{k_1}{2.303} t$$

In the formula, q_t represents the adsorption amount at time t, mg/g; q_e represents the adsorption amount at equilibrium, mg/g; k_1 represents the first-order adsorption rate constant, min^{-1}; t represents the adsorption time, min.

The second-order reaction rate equation is:

$$\frac{t}{q_t} = \frac{1}{k_2 q_e^2} + \frac{1}{q_e} t$$

Adsorption data for Cu^{2+}, Cu-NH_3, Cu-Cit, and Cu-EDTA were fitted using Lagergren's first and second-order reaction rate equations. The first and second-order reaction kinetics curves are shown in Figure 5, and the parameters are listed in Table 6. As can be seen from the table, compared to the Lagergren first-order reaction rate kinetics curve, the second-order adsorption kinetics model for the adsorption data of Cu^{2+}, Cu-NH_3, Cu-Cit, and Cu-EDTA using coal gasification ash activated carbon has a higher degree of fit, with the linear correlation coefficients (R^2) being 0.970, 0.980, 0.964, and 0.994, respectively.

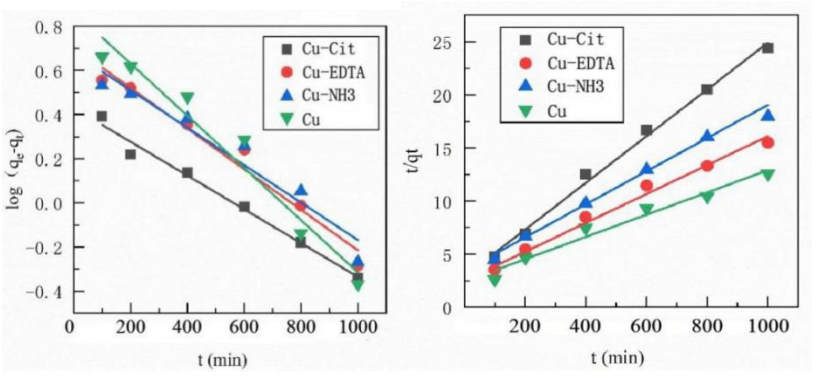

Figure 5: First-order (a) and second-order (b) adsorption kinetics curves for the adsorption of Cu^{2+}, Cu-NH_3, Cu-Cit, and Cu-EDTA.

Table 6: Isotherm parameters for the adsorption of Cu^{2+}, Cu-NH_3, Cu-Cit, and Cu-EDTA by coal gasification ash activated carbon.

Adsorbent	Pollutant	q_e mg/g	Lagergren first-order kinetics			Lagergren second-order kinetics		
			k_1 min^{-1}	$q_{e,c}$ mg/g	R^2	k_2 min^{-1}	$q_{e,c}$ mg/g	R^2
AC	Cu^{2+}	40.56	0.0273	35.66	0.9863	0.0044	46.75	0.9700
AC-EDTA	Cu-EDTA	36.67	0.0214	28.02	0.9690	0.0073	37.50	0.9807
AC-NH_3	Cu-NH_3	29.11	0.0195	28.25	0.9437	0.0070	36.27	0.9641
AC-Cit	Cu-Cit	24.38	0.0175	14.55	0.9571	0.0164	23.65	0.9949

3.6 The effect of pH value on adsorption experiments

Figure 6 illustrates the adsorption behavior of gasification ash activated carbon on Cu^{2+}, Cu-NH_3, Cu-Cit, and Cu-EDTA at varying pH levels. From the graph, we observe that as the pH gradually increases, the adsorption capacity of the adsorbent for both Cu2+ and complexed copper initially increases and then decreases.

At pH values below 5, the solution contains a significant number of hydrogen ions. These ions

ISSN 2616-5880 Vol. 5, Issue 2: 37-45, DOI: 10.25236/AJMC.2024.050207

compete with Cu^{2+}, Cu-NH_3, Cu-Cit, and Cu-EDTA for adsorption sites on the surface of the gasification ash activated carbon. The hydrogen ions occupy active sites, hindering the adsorption of the copper species. As the pH rises beyond 5, the concentration of hydrogen ions decreases, and hydroxide ions increase. This change may lead to preferential binding with Cu^{2+}, Cu-NH_3, Cu-Cit, and Cu-EDTA, resulting in reduced adsorption capacity.

Interestingly, at pH 5, the gasification ash activated carbon exhibits maximum adsorption capacity for Cu^{2+}, Cu-NH_3, Cu-Cit, and Cu-EDTA.

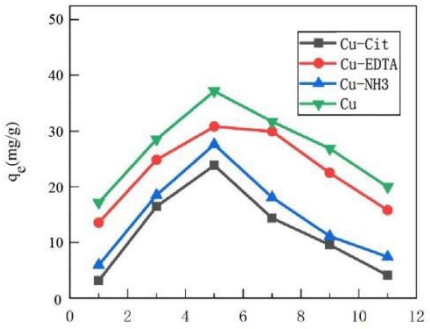

Figure 6: Adsorption of AC residue on Cu^{2+}, Cu-NH_3, Cu-Cit, and Cu-EDTA at different pH values.

3.7 Impact of adsorbent dosage on adsorption experiments

Figure 7 illustrates the adsorption behavior of gasification ash activated carbon on Cu^{2+}, Cu-NH_3, Cu-Cit, and Cu-EDTA at varying dosages. As shown in the graph, with increasing adsorbent dosage, the available adsorption surface area and active sites provided by the adsorbent also increase. However, the concentration of Cu^{2+}, Cu-NH_3, Cu-Cit, and Cu-EDTA in the solution remains constant. Consequently, the unit adsorption capacity decreases as the adsorbent dosage increases. Therefore, as the dosage increases, the adsorption capacity for Cu^{2+}, Cu-NH_3, Cu-Cit, and Cu-EDTA all exhibit a decreasing trend. Considering experimental uncertainties, the optimal adsorbent dosage for Cu^{2+}, Cu-NH_3, Cu-Cit, and Cu-EDTA corresponds to a range between 20 and 100 mg, with the maximum adsorption capacity achieved at a dosage of 20 mg.

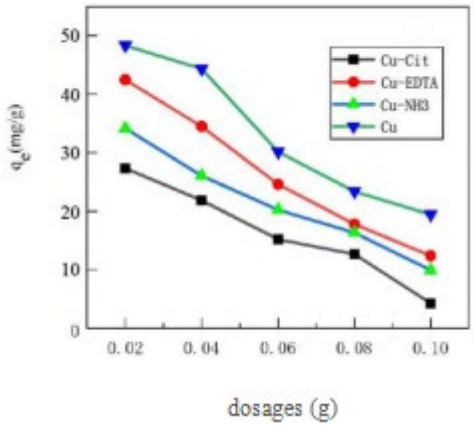

Figure 7: Adsorption of AC residue on Cu^{2+}, Cu-NH_3, Cu-Cit, and Cu-EDTA at different dosages.

3.8 X-Ray diffraction pattern

The Figure 8 XRD diffraction patterns of coal gasification ash activated carbon reveal that AC, coal gasification ash activated carbon-Cu-EDTA (AC-Cu-EDTA), coal gasification ash activated carbon-Cu-Cit (AC-Cu-Cit), and coal gasification ash activated carbon-Cu-NH_3 (AC-Cu-NH_3) all exhibit several independent, narrow, sharp peaks. This indicates that these samples are well-crystallized substances, primarily existing in an amorphous form. Notably, within the 2θ range of 20~30°, some peaks in the coal gasification ash activated carbon become significantly broader, suggesting that the crystal particle size in the sample is less than 300 nm. The characteristic diffraction peaks of SiO_2 are

ISSN 2616-5880 Vol. 5, Issue 2: 37-45, DOI: 10.25236/AJMC.2024.050207

also distinctly observed, indicating a substantial proportion of SiO_2 in the components of the coal gasification ash activated carbon.

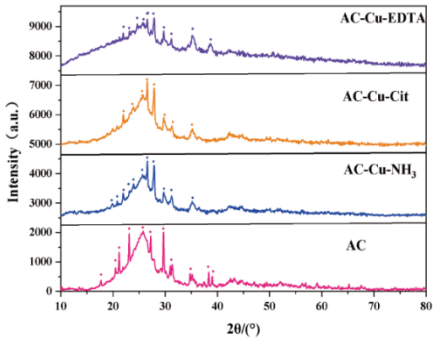

Figure 8: X-Ray Diffraction Pattern of AC, AC-Cu-EDTA, AC-Cu-Cit, and AC-Cu-NH_3.

3.9 Fourier transform infrared spectroscopy

The infrared spectrum of AC, AC-Cu-EDTA, AC-Cu-Cit, and AC-Cu-NH_3 shows a broad characteristic peak at approximately 3430 cm^{-1} Figure 9. This is likely due to the stretching vibrations of O-H and C-C bonds. A weaker peak at 2928 cm^{-1} may be attributed to the bending vibrations of O-H bonds, suggesting that these samples may contain a large amount of adsorbed water or functional groups with hydroxyl groups. Additionally, a distinct peak at approximately 1060 cm^{-1} could be due to the anti-symmetric stretching vibrations of SiO_2, indicating the presence of Si-O functional groups in these samples.

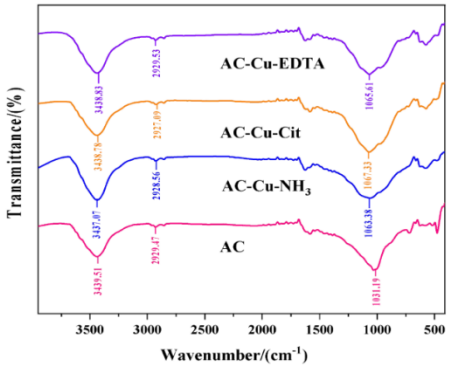

Figure 9: Infrared Spectra of AC, AC-Cu-EDTA, AC-Cu-Cit, and AC-Cu-NH_3.

4. Conclusion

This study investigates the adsorption properties of AC for Cu^{2+}, Cu-NH_3, Cu-Cit, and Cu-EDTA. It examines the effects of various factors such as adsorbent dosage and pH on the adsorption process. The research employs adsorption kinetics and isotherm models to explore the adsorption process and reveal its mechanism. Additionally, various characterization techniques are used to describe the pore structure of AC. SEM images reveal that AC primarily exhibits an irregular glassy phase, with a rough surface texture and a certain amount of porosity; it also contains a mixture of spherical particles. The surfaces of these spherical particles are relatively smooth, mainly because they are formed under high-temperature melting conditions. BET surface area analysis indicates that AC possesses a rich pore structure, which mainly originates from incompletely combusted carbon within the material. EDX spectroscopy and elemental analysis show that carbon is the predominant element in AC, playing a leading role in the adsorption process and contributing to a significant adsorption effect. XRD diffraction patterns suggest that the samples of AC are well-crystallized substances. FTIR spectra display three distinct peaks, likely due to the stretching vibrations of O-H, C-C, and aromatic C-H bonds.

ISSN 2616-5880 Vol. 5, Issue 2: 37-45, DOI: 10.25236/AJMC.2024.050207

References

[1] Wang J B, Xu Z M. Disposing and Recycling Waste Printed Circuit Boards: Disconnecting, Resource Recovery, and Pollution Control [J]. Environmental Science & Technology, 2015, 49(2): 721-33.

[2] Zhang L, Wu B D, Gan Y H, et al. Sludge reduction and cost saving in removal of Cu(II)-EDTA from electroplating wastewater by introducing a low dose of acetylacetone into the Fe(III)/UV/NaOH process [J]. Journal of Hazardous Materials, 2020, 382.

[3] Zhang J Z, Wang Z Q, Zhao R D, et al. Gasification of Shenhua Bituminous Coal with CO_2: Effect of Coal Particle Size on Kinetic Behavior and Ash Fusibility [J]. Energies, 2020, 13(13).

[4] Zhou S L, Wei W D, Chen L, et al. Impact of a Coal-Fired Power Plant Shutdown Campaign on Heavy Metal Emissions in China [J]. Environmental Science & Technology, 2019, 53(23): 14063-9.

[5] Guo F H, Chen L Q, Li Y, et al. Review on the attribute cognition and carbon-ash-water separation of coal gasification fine slag [J]. Separation and Purification Technology, 2023, 320.

[6] Gollakota A R K, Volli V, Shu C M. Progressive utilisation prospects of coal fly ash: A review [J]. Science of the Total Environment, 2019, 672: 951-89.

[7] Xu L, Liu Y N, Wang J G, et al. Selective adsorption of Pb^{2+} and Cu^{2+} on amino-modified attapulgite: Kinetic, thermal dynamic and DFT studies [J]. Journal of Hazardous Materials, 2021, 404.

[8] Das K C, Garcia-Perez M, Bibens B, et al. Slow pyrolysis of poultry litter and pine woody biomass: Impact of chars and bio-oils on microbial growth [J]. Journal of Environmental Science and Health Part a-Toxic/Hazardous Substances & Environmental Engineering, 2008, 43(7): 714-24.

[9] De Carvalho T E M, Fungaro D A, Izidoro J D. Adsorption of reactive orange 16 from aqueous solutions by synthesized zeolite [J]. Quimica Nova, 2010, 33(2): 358-63.

[10] Bhattacharyya K G, Sen Gupta S. Influence of acid activation on adsorption of Ni(II) and Cu(II) on kaolinite and montmorillonite: Kinetic and thermodynamic study [J]. Chemical Engineering Journal, 2008, 136(1): 1-13.

[11] Chai Z, Lv P, Bai Y H, et al. Low-cost Y-type zeolite/carbon porous composite from coal gasification fine slag and its application in the phenol removal from wastewater: fabrication, characterization, equilibrium, and kinetic studies [J]. Rsc Advances, 2022, 12(11): 6715-24.

[12] Liu L, Jiao Q R, Yang J, et al. Influences of Ash-Existing Environments and Coal Structures on CO_2 Gasification Characteristics of Tri-High Coal [J]. Processes, 2020, 8(11).

[13] Shahabuddin M, Kibria M A, Bhattacharya S. Evaluation of high-temperature pyrolysis and CO_2 gasification performance of bituminous coal in an entrained flow gasifier [J]. Journal of the Energy Institute, 2021, 94: 294-309.